AIRCRAFT PATH EXTRACTION FROM NOISY TARGET DATA

Sergio Torres, Ph.D.
Lockheed Martin Transportation and Security Solutions
9211 Corporate Blvd. Rockville, MD 20850
USA
sergio.torres@lmco.com

ABSTRACT
Testing of air traffic control (ATC) and air traffic management (ATM) systems benefits from the availability of realistic scenario data based on live recorded traffic. The difficulty with such data sets is the dependency on local geography and adaptation of the site where the data was collected. Scenario data is typically used in an environment different than the original, potentially with new sensor types and configuration. An example is the evaluation of the accuracy of the tracking and conflict alert functions for future systems that plan to implement data fusion of radar and automatic dependent surveillance-broadcast (ADS-B) data using a scenario based on data where only radar surveillance is available today. This paper presents an algorithm to extract "ground truth" from live recorded data such that the noiseless aircraft paths are obtained with their relative separations preserved and in a representation decoupled from the sensor types and the geographic configuration specific to the originating site. Ground truth obtained from the path extraction (PE) algorithm can be used as input to target generation software configured for a specific sensor environment as required for the system under test.

The PE algorithm is basically a maneuver detector that looks for changes above noise in heading, altitude, speed and vertical velocity. The algorithm relies on identifying those segments where the relevant kinematic data (heading, altitude, horizontal and vertical speed) could be considered constant and consistent with noise. Unlike a purely statistical change detector, which is more sensitive to the correct modeling of noise, the PE algorithm is more robust because the straightforward geometric approach that it uses looks at the overall effect of a maneuver rather than trying to detect the point where the maneuver takes place. For example, a small change in heading is difficult to detect when looking for the maneuver point, but the change it produces is easily recognized by examining the entire realized track. The horizontal component of the extracted aircraft paths are expressed in stereographic coordinates on a common surveillance system plane. It is shown that, together with aircraft altitude, this choice of coordinate system lends itself to relocate the traffic easily to any region on the ellipsoidal Earth. The PE algorithm provides segmented aircraft path data, which in addition to its use to generate reference scenarios for testing, can also be used to infer aircraft intent, to obtain scenario characterization metrics, and for detection of the phase of flight. Metrics to evaluate the performance of the PE algorithm are presented and results of an evaluation are discussed.

KEY WORDS
scenario data, maneuver detection, aircraft path extraction, change detection, aircraft intent inference.

1. Introduction

Testing and validation of components for air traffic management (ATM) systems rely on the availability of suitable scenario data. In the area of trajectory prediction the Action Plan 16 group has identified the need for reference scenario data for validation of current and future applications [1]. Current efforts by the Federal Aviation Administration (FAA) to implement automatic dependent surveillance-broadcast (ADS-B) in the national airspace system (NAS) present challenging testing and validation needs requiring the availability of reference scenarios that can be applied across a wide range of new and legacy platforms. Evaluating the performance of tactical alert functions with real-world data is yet another example that highlights

the need for reference scenario data. In order for such scenario data to be useful it should be realistic, independent of sensor type, and not tied to a particular geographic adaptation. This paper presents a scenario data generation solution that addresses these three points. The approach is to start from recorded radar data (hence realistic), extract from these recordings an approximation of the 4D paths followed by the aircraft (or "ground truth"), which is independent of sensor characteristics and expressed in a coordinate system that can easily be translated to any location on the geodetic Earth. In this approach it is envisioned that the scenario data consists of 4D aircraft paths and that the system where the scenario is going to be used has target generation software that receive as input these 4D paths and it is configured for the relevant sensor environment of the test.

The technique to extract the aircraft path from noisy targets consists of identifying changes above noise in any one of the dimensions of course angle, altitude, speed, or vertical speed and building segments accordingly. The algorithm decomposes the observed sequence of target reports into separated stationary segments. The desire is to obtain a noise-free path that preserves the realism of the aircraft motion in 4D to a controlled level of fidelity. Smoothing filters cannot be applied with high strength because they deform the path and will always leave residual noise. Maneuver detection point algorithms that use standard statistical hypothesis testing [2] do not work well because of the quantization of radar target data (especially in the altitude dimension) and because of difficulties to correctly formulate the noise model in a multisensor environment. Spline and curve fitting methods suffer from discontinuities at the joins of successive segments. Locally weighted polynomial regression or LOESS filtering [3] also is not satisfactory in aircraft path reconstruction because 1. it does not accept high order polynomials; 2. it cannot deliver a solution in a form readily usable for segment identification; and 3. being derived from the Least Squares formalism it is sensitive to the accuracy of the noise model, which is nontrivial in a multisensor environment. The method proposed here overcomes these difficulties by building segments (in any of the above mentioned dimensions) via a process of point decimation that removes data points that do not add information because they are deemed consistent with noise. The algorithm looks at the effect of a maneuver instead of trying to identify the maneuver point, although the maneuver point will be a byproduct. Details of the algorithm are presented in Section 3.

In addition to the direct benefit of scenario data generation provided by the PE algorithm there are a number of applications that derive from it: scenario metrics, detection of the phase of flight [4], inference of aircraft intent.

Another problem one encounters in generating reference scenario data for testing is the need to express "ground truth" in such a way that it makes it easy to reuse in systems with geographic adaptation different than that where the original data was recorded. A data representation method is developed and potential accuracy losses because of coordinate transformations are quantified, as detailed in Section 4.

2. The Statistics of Change Detection

Within the context of the algorithm presented here, recorded radar data consists of the reported horizontal position, the Mode C altitude and the associated time. In order to combine the targets for an aircraft from multiple sensors the horizontal positions are stereographically projected to a common system plane. Working on the Eucledean plane has the additional advantage of substantially simplifying the geometric computations that the algorithm needs. Nominal Gaussian noise in slant-range (ρ) and azimuth (θ) combined with quantization, potential uncorrected registration bias and uncompensated time latencies affecting time stamping, result in noise distributions for the horizontal position on the system plane that exhibit high kurtosis. Furthermore, whereas jitter noise in the native coordinates (ρ,θ) is uncorrelated, it will be correlated in the XY coordinate system on the common system plane.

The situation at hand is one where it is desired to extract a 'signal' that has been contaminated with noise of complex characteristics. The 'signal' in this case is the actual path of the aircraft which could include small deviations from steady state (transients) as well as slowly varying changes. Observed data exhibits variations from steady state resulting from a superposition of a deterministic component and a noise component. The goal of the path extraction algorithm is to recover the deterministic part of the data.

Note that by virtue of the fact that we are dealing with recorded data the problem is of an *off-line* nature, thus the advantages of *acausal* filtering can be exploited. Detection of short maneuvers is limited

by the sampling theorem, effectively preventing detection of maneuvers that occur within a time shorter than the inverse of the Nyquist critical frequency.

In typical statistical change detectors applied to a time series [2], a sliding window of n points is used to evaluate a statistic parameter (for instance the average). The parameter is computed before and after a test point, if the difference in the parameter exceeds a suitably set threshold (for example based on Student's t-distribution for averages) then the null hypothesis (that there is no change) is rejected. The performance of this method is limited by the ability to provide an accurate noise model which is problematic because of the above mentioned complexities for a mix of targets projected on a plane.

A more effective approach to change detection is to look at the entire realized track where the effects of maneuvers will be visible by the total deviation from steady state. Consider course angle: a small turn in the middle of the track is going to cause, downstream, a large transverse deviation relative to the direction prior to the turn. The section that follows explains how this geometric approach works.

3. The PE Algorithm

The path extraction (PE) algorithm works in two types of data sets: time series and XY data. Altitude and velocity are treated as a time series and horizontal position as XY data. Segmentation of time series is described first and then the method is generalized for horizontal segmentation on the Eucledean plane.

Prior to using the targets for segmentation, target selection and smoothing of the raw target data is performed. Target selection is the process of discarding outliers (possibly due to duplicate beacon codes) and targets that come too close together in time. There is no useful information in a target that comes within a time from the previous target of $\Delta t < \mathrm{Max}(\sigma_\rho, \rho\sigma_\theta)/v$, where v is the velocity of the target, ρ the target range, and σ_ρ, σ_θ the nominal standard deviations for range and azimuth noise. Removal of outliers should be considered in the event of known data collection artifacts (such as invalid Mode C data points). Unique aircraft identification schemes (using beacon code, aircraft ID or a combination) should be established according to the aircraft information available in the recordings. A pass of a very mild smoothing filter before targets are use for segmentation can reduce noise power with minor deformations of the paths. This operation helps in reducing the variance of the derived velocities. The advantages of acausal time domain filtering are exploited to produce smoothing without introducing time lag. The convolution of the X_k and Y_k time series separately with an impulse response function given by a truncated Gaussian provides a smoothing function which can be easily adjusted to control the desired behavior. The two parameters of a truncated Gaussian, width σ_s and cut-off c_s, can be adjusted to produced a moving average filter ($\sigma_s >> c_s$) or regular Gaussian smoothing ($c_s >> \sigma_s$).

Time series segmentation: Let q_k be a time series of the relevant variable, for example altitude or horizontal velocity, and let D be the fidelity criteria defining the scale of the smallest variation that we want to retain. Time is represented by the discrete index k (k: 1,2,3,…n). The fidelity parameter D should be a small factor of the RMS noise amplitude or the quantization interval, whichever is the largest. The results are not too sensitive to D, as long as it is higher than noise level. The algorithm removes points on the time series that do not deviate by more than a distance D from a linear trend through the points.

Define the deviation $d_k(s,m)$ as:

$$d_k(s,m) = \left\| q_k - Q(k;s,m) \right\| \tag{1}$$

where, q_k is the value of the k-th point in the series, Q(k;s,m) is the value of the function Q evaluated at the k-th time, Q being the straight line joining the series points q_s and q_m as illustrated in Figure 1. The interval [s,m] defines a search window. Initially the starting points are set to s = 1, and m = n. Both are marked as nodes. Segment identification proceeds in a loop as follows:

- start
- Compute M = MAX(d_i(s,m)), i: s → m;
- if the condition M < D is satisfied, mark the point i = m as a node; set s = m; set m = n; if s equals n exit the loop, else go to the star of the loop;
- else, decrease m (m = m - 1) and go to the start

The nodes mark the start and end points of the segments that have been identified. The location of the edge of the segment can be refined as described below. In the example shown in Figure 1 there will

be 3 segments left ([s,a], [a,b], and [b,m]) after removing all those points not marked as nodes.

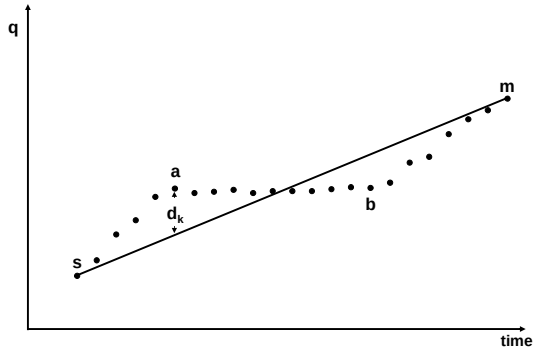

Figure 1. Time series example

Horizontal segmentation is done with the target data projected on a common stereographic plane. This step is not only necessary to combine the positions reported by multiple radars but also simplifies the geometric calculations required by the algorithm and provides a natural coordinate system that allows redeployment of the data at a different location as explained in Section 4. Segmentation along the XY plane follows a similar approach to the time series segmentation with the difference that d_k is now defined as the Eucledean distance between the point (x_k,y_k) and the perpendicular projection of this point on the straight line joining the points (X_s,Y_s) and (X_m,Y_m) as shown in Figure 2. The interval [s,m] defines the search window as before. Note that segmentation of both time series and horizontal XY data does not required that sampling in time be uniform and for XY data it is tolerant of artifacts such as heading reversals caused by combining high-noise targets from multiple radars. For the horizontal path, the choice of performing segmentation directly on XY data rather than the option of applying the segmentation algorithm on the heading angle time series stems from the fact that in building the heading angle time series the computation introduces large errors due to the propagation of horizontal position errors.

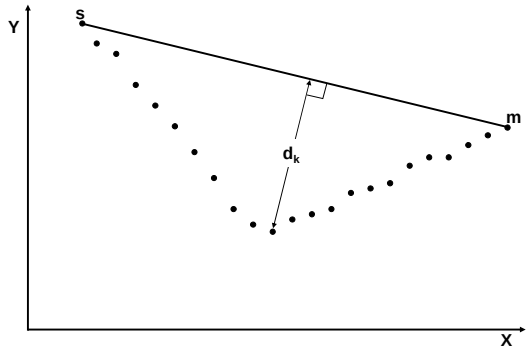

Figure 2. Sample X-Y data

Refinement of segment edges to obtained segments closer to the data points can be done by computing the sum of the residuals:

$$\chi^2 = \sum d_k^2(s,m) \qquad (2)$$

for m (the node at the end of the segment) varying few points before and after the original point found for the edge. The choice of m that minimizes χ^2 would provide the optimal fit in the Least Squares sense. For the particular case of Mode C data which has a quantization interval (r = 100 feet, usually) larger than the effective RMS of the data, detection of departures from level and level off points on the vertical profile can be adjusted for a better identification of the edges by checking the neighboring altitudes points and moving the edge to the last altitude point with the same altitude value as the altitude of the level segment prior to the start or after the end of the altitude transition.

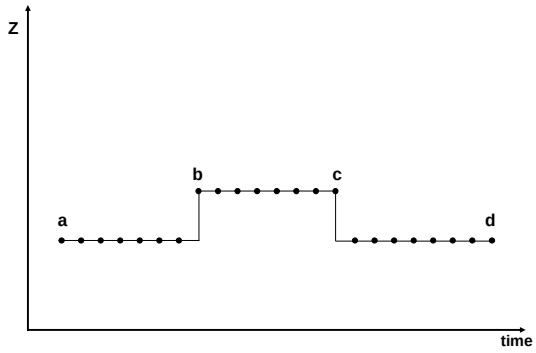

Figure 3. Vertical profile example

For Mode C altitude data there is an additional step in the process of segmentation due to the need to

detect excursions from level. Consider the vertical profile in Figure 3 with a level segment [a,d] that includes an excursion [b,c]. Mode C altitude data is characterized by level segments and altitude transitions. A long level segment however can have excursions to an altitude ±r around the level altitude. In this case the fidelity parameter D should be set to a value greater than r. With D > r, the segmentation algorithm will flag points a and d as nodes leaving segment [a,d] as the only solution, thus the excursion [b,c] goes undetected. Observation of recorded data shows that during a phase of flight where the aircraft is level the Mode C reported altitude is consistently constant over long stretches of time and that if any deviations occur these deviations tend not to exhibit the properties of uncorrelated noise. Rather they show step-wise correlated excursions. This suggests that the observed deviations originate from actual motion of the aircraft in altitude toward one of the levels inside the quantization interval rather than from altimeter jitter. From the formalism of random excursion sets [5] one can specify the characteristics of excursions in terms of the mean lengths of the excursions and of the gaps in between them.

To detect excursions the PE algorithm includes post-processing of altitude segments flagged as level consisting of searching for instances of a run of N_e consecutive Mode C data points that deviate by +r or -r from the segment altitude followed by a run of N_h data points (a gap) with altitude at the level of the segment. The N_e and N_h parameters are fined tuned with empirical data.

Because the topic of this paper bears on simulated target generation it is important to point out a correction to the common misconception that Mode C noise is white noise and that quantization can be modeled as a separate noise component with $\sigma = r/\sqrt{12}$ (r = quantization interval, and the square root comes from the uniform distribution assumption). This recipe not only results in excess noise (quantization reduces the variance of the data) but also with uncorrelated noise, which is not the case. This is because the altimeter noise is considerably smaller than quantization and the Mode C sensor is not in the radar but instead it is the altimeter on board the aircraft, thus the radar scan period has nothing to do with the operation of the altimeter. In generating Mode C data it is the effect of excursions and not sensor noise what is most relevant. Deviations from level should be modeled as excursions of value ±r and gaps in between, with the respective lengths of excursions and gaps that follow exponential distributions.

Observation of 6 hours of recorded Mode C data in the en-route portion of the flight shows that the excursion and gap lengths follow distributions significantly different than those expected from uncorrelated noise (Equation (4)). The observed durations of gaps and excursions fit an exponential distribution with widths equal to 6 sec (gaps) and 60 seconds (excursions). These results are significantly different than what would be expected from white noise. Under the uncorrelated random noise assumption, for altimeter data with noise level smaller than the quantization interval ($\sigma < r$) the probability of observing a Mode C report exceeding r for a level segment is

$$p_e = P(z > r) = 2(1 - F(\frac{r}{t\sigma})) \qquad (3)$$

where F(z) is the cumulative normal distribution function and t = 1 if the quantization operator truncates, 2 if it rounds up. The excursion probability density function for Gaussian white noise is

$$E(n) = (1-p)\,p^{n-1}, \quad n : 1...\infty \qquad (4)$$

where,

E(n) is the probability of an excursion (using $p = p_e$) or gap (using $p = 1 - p_e$) of length = n points; r = quantization interval, p_e = probability of one point excursion (Equation (3)).

Because segmentation is performed separately along the horizontal, altitude and velocity dimensions the nodes from each dimension need to be 'merged' to build the final segment. Changes in vertical velocity will appear as breakpoints (nodes) in the vertical segmentation. The result of segmentation is contained in an array with dimension equal to the number of targets. This array stores node information: if a point is a node in either dimension it will have a non-zero entry. Final segments are built by first removing all those points that are not marked as nodes, then adjusting the XY coordinates of the points not marked as XY-nodes (i.e. they are nodes in velocity or altitude) so that they lie along the line segment joining the nearest XY-nodes at the point of the perpendicular projection. The latter operation is to guarantee that horizontal segmentation is not affected by velocity or altitude nodes. For example, consider a straight horizontal segment with a change in velocity in the middle. The velocity maneuver point is properly marked as a

velocity node which means that the target corresponding to that node (i.e. a target and all its attributes: position, altitude, time, etc) will not be removed. After removal of all the targets not marked as nodes we end up with three targets: the start and end of the original horizontal segment and a target in the middle accounting for the velocity maneuver point. The XY coordinates of the target associated with the later node are subject to noise and thus are not expected to lie along the straight segment. That is why they are adjusted to the perpendicular projection point.

The final pass of the PE algorithm consists of resampling followed by a smoothing operation to obtain a realistic rendering of turns. The horizontal segmentation operation delivers straight segments joined at the nodes, the horizontal speed (V) and heading change angle (β) at a node are obtained from the geometry of the path and are available to parameterize the turn. The target generation software using the PE paths can model the turn with the turn parameters V and β (for example assuming a fixed bank angle (α), the radius of the turn is R = $V^2/g \tan\alpha$ and the duration of the turn T = Rβ/V). A more practical rendering of the turns is obtained by applying a pass of the Gaussian smoothing filter to resampled data. With resampled data at suitable time intervals the demands on the target generator are straight forward because they only need to time interpolate along straight segments. The sampling step and strength of the smoothing are empirically tuned by comparing the resulting turn with a coordinated turn at a fixed bank angle. The error in turn modeling relative to a coordinated turn is:

$$\delta = \frac{V}{\omega}(1-\cos(\frac{\omega\tau}{2})) \tag{5}$$

where V is the tangential velocity, ω is the angular velocity, τ is the sampling time and δ the maximum deviation between the approximated segment and the arc along the true curved path inside the turn. A useful expression for δ, taking into account units and using the small angle approximation is:

$$\delta = \frac{\pi\omega\tau^2}{12960}\left(\frac{V}{400\ knots}\right) \tag{6}$$

where V is in knots, ω in °/sec, τ in sec and δ in nmi. With τ = 6 sec and reasonable values for cruise phase of V and ω of 400 knots and 1 °/sec respectively, one obtains δ = 0.0087 nmi (~ 53 feet) which is well below the horizontal fidelity level. It is observed that the smoothing parameters can be made optimal depending on the amplitude of the course angle change, which suggests that the PE extraction can be applied in batches of different aircraft types (military, general aviation, commercial, etc) whose paths generally exhibit different horizontal maneuvering patterns and PE parameters can be individually optimized for each group.

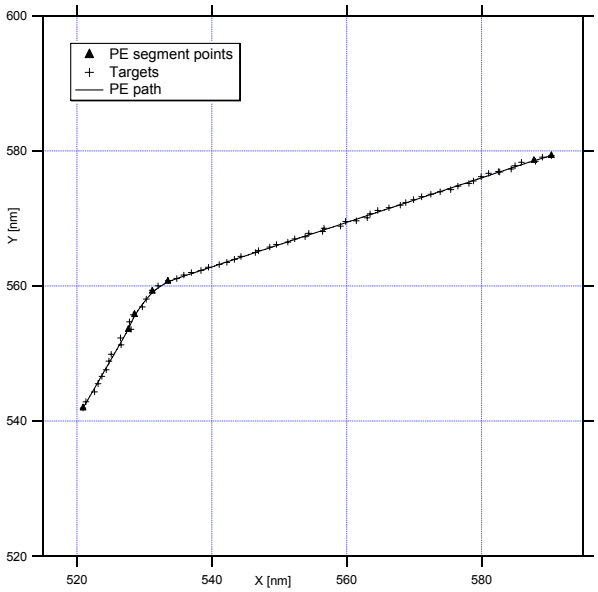

Figure 4. Example of PE extracted path

Figure 4 shows the results of applying the PE algorithm to a sample of synthetic radar data generated from known truth consisting of two straight segments joined by a 42° turn (at 1 °/sec). As can be seen from the plot, the 64 targets were reduced to just 7 points, 4 defining the long segments and the remaining defining the turn. The goal of separating the non random component of the data has been achieved. The end results of PE algorithm are constant velocity segments. The attributes of segment end points are: horizontal position, altitude and time. Velocities are implicit and acceleration results in a sequence of smaller segments each with different constant velocity.

4. Coordinate System Transformations

Once we have a collection of 4D aircraft paths it is desired to be able to take that traffic and place it centered on top of a site at an arbitrary location. The ability of generating "reference" scenarios hinges on complying with the requirement of providing the data in a geography independent format that preserves the relative positions of the aircraft.

Specifying horizontal positions using latitude and longitude for a reference scenario does not work well because it is tied to a geographic location. An alternative would be to express the points defining the aircraft path in an Earth centered - Earth fixed (ECEF) coordinate system and then applying a rotation of the unit vectors using the Euler angles [6]. This solution would require additional coordinate transformations and it is not immune to the dilation error explained below. If the extent of the traffic included in the scenario is less than 4000 - 5000 nmi a more practical solution is to express the horizontal position of the segment end points of an aircraft path in XY Cartesian coordinates on the working stereographic plane. Since the points are already available in that coordinate system, one can save a few transformations. Redeploying the traffic on the target site is accomplished by moving the point of tangency (POT) of the stereographic plane (presumably chosen to lie near the center of gravity of the traffic) to the new desired location, then projecting the points back to the conformal sphere and to the Earth's ellipsoid. The end result is that the horizontal positions are now available in geodetic coordinates relative to the target site (altitude above the ellipsoid is not transformed). As long as the radius of the conformal sphere is maintained constant the relative aircraft positions will be preserved, except for a negligible dilation or contraction that occurs as a result of the POT change explained below.

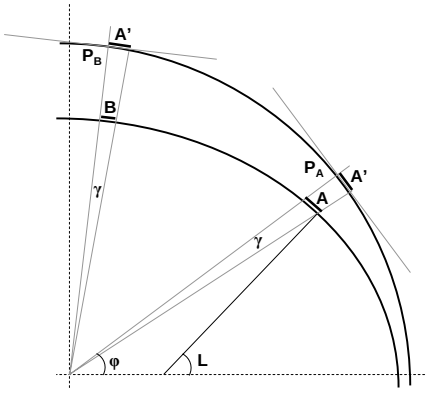

Figure 5. Stereographic projection

A small error in relative distances is introduced when the latitude of the POT is changed. The origin of this error is the fact that whereas the length of the arc on the conformal sphere subtended by a fixed angle γ (with vertex at the center of the Earth as shown in Figure 5) is constant, the same angle subtends an arc along the ellipsoid that depends on latitude. Figure 5 shows a segment on the meridional ellipse (segment A) parallel to the meridian and subtending an angle γ from the center of the Earth. The projection on the conformal sphere is approximately indicated with the arc A′ (the conversion from geodetic latitude to conformal latitude does not have a straightforward geometric interpretation, as it depends on latitude). If we move the POT from P_A to a different latitude P_B one can see that the projection on the ellipsoid (B) has different length that the original segment A. One would expect segment B to be shorter than segment A because the angle γ remains constant but B is closer to the center of the Earth than A. Moving the POT to a different longitude does not introduce dilation errors.

To find the magnitude of dilation (or contraction) errors one only needs the dilation factor k_1 in going from ellipsoidal to conformal. Let A, A′, and B denote the lengths of the respective segments. In this case this factor is $k_1 = A'/A$ and is given by [7]:

$$k_1 = \frac{R\cos\phi\sqrt{1-\varepsilon^2\sin^2 L}}{R_q\cos L} \tag{7}$$

Where:

R = radius of the conformal sphere
R_q = equatorial Earth radius
ε = eccentricity of ellipsoid
L = geodetic latitude of POT
ϕ = latitude L converted to conformal

By combining the dilation factor for two transformations, namely from ellipsoidal to conformal (k_1: A → A′) to put the raw data on the stereographic plane and then from the new conformal (POT moved tp P_B) back to ellipsoidal (k_1': A′ → B), the total dilation factor is $k_0 = k_1'/k_1$)

$$k_0 = \frac{k_1'}{k_1} = \frac{A'/B}{A'/A} = \frac{A}{B} \tag{8}$$

Thus, using Equation (7) and after some algebra:

$$k_0 = \frac{\cos\phi'\cos L\sqrt{1-\varepsilon^2\sin^2 L'}}{\cos\phi\cos L'\sqrt{1-\varepsilon^2\sin^2 L}} \tag{9}$$

Where the primed variables correspond to the latitudes of the POT after it has moved to the new location. The difference in length A - B = A(1 - $1/k_0$) is the error in the distance separating two points when the POT is translated to another latitude and

Figure 6 shows a plot of this error as a function of how far in latitude the POT has been moved. In the plot the error is in units of 1-thousandth of an nmi. We started with an initial L = 45° but the shape of the curve and the difference between the maximum and minimum error (which is 1/100 nmi) does not change.

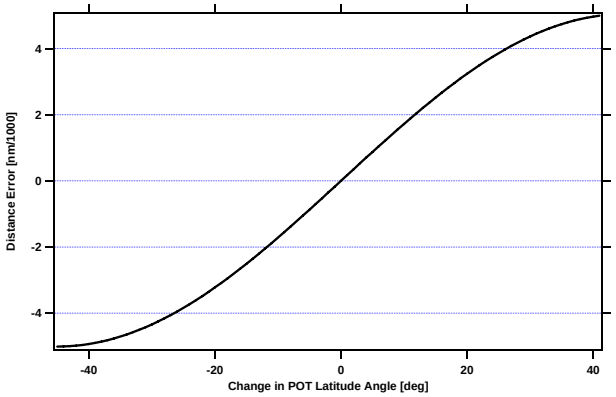

Figure 6. Dependence of error in distances as the point of tangency is moved in latitude

The maximum error (~1/100 nmi as noted) would be injected when data originally recorded at a site with L = 0° is redeployed to a site with L = 90°. Around the center (L = 45°) the curve is symmetric and linear (error ~ 1 foot per each 1° displacement in POT latitude). The error does not depend on the choice of conformal radius (which must be maintained constant) or distance of the data points from the POT. The latter is valid because transformations from conformal to stereographic and back to conformal preserve the distances on the conformal sphere, no matter how far from the POT.

5. Algorithm Evaluation

To evaluate the PE algorithm an end-to-end test was performed consisting of comparing extracted 4D aircraft paths with the *ad hoc* aircraft paths from which targets were generated. The steps involved in the test, from data preparation to metrics computation, are described below.

We started with a set of 467 flights whose 4D noiseless paths are known. This set of input paths is based on actual recorded data (~ 2 hours) but how exactly the paths were obtained is not necessary to know because they are the starting point of the chain (i.e. we use these paths as the known truth). Radar configuration consisting of 17 radars (4 short and 13 long range) was put in place for the target generation tool (the EG tool). EG generates targets based on the radar scan time (4.7 sec for short range and between 10 and 12 sec for long range). The tool was configured to add Gaussian noise to the azimuth (σ_θ = 1.6 ACP and 1.4 ACP) and slant range (σ_ρ = 0.05 and 0.025 nmi) with standard deviations as indicated for long and short range radars respectively. Range and azimuth is quantized and a blip-scan ratio 0.95 is applied. The generated targets were used as inputs to the PE algorithm, which was run with configuration parameters set as shown in Table 1

Table 1. PE parameters for test run

Parameter	Value	Units
MinTargetGap	3.0	sec
XYSmoothGaussian	9	sec
XYSmoothCut	3.5σ	
FidelityXY	0.2	nmi
FidelityV	75.0	knots
FidelityZ	101	feet
Resample	6	sec
LevelDeviation	101	feet
LevelTimeWindow	60	sec
MaxExcursionGap	12	sec
MinExcursionLength	42	sec

The performance of the PE algorithm has been measured in terms of the RMS horizontal deviations of the PE extracted paths relative to the true paths and the residual noise in the PE paths. The horizontal position RMS deviations of the PE paths (uniformly sampled with a 6 sec sampling time) relative to the true paths is 0.22 nmi consistent with the 0.2 nmi setting of the horizontal fidelity parameter. Similarly, the measured altitude deviation RMS is 26 feet. Lowering the fidelity parameter should reduce the value of this metric, but at the expense of increased residual noise.

The deviations of target horizontal position around the aircraft path were computed relative to both the known true input paths (from which targets were generated) and the PE extracted paths. The distributions of this metric should reveal the amount of effective target noise (Figure 7), thus when measured against the PE extracted paths the distribution should closely follow the shape that results when measured against the true paths. Any difference in shape reveals residual noise in the PE tracks.

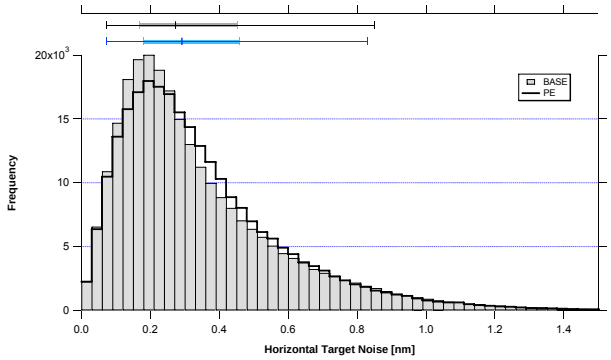

Figure 7. Effective horizontal target noise relative to known true (solid bars) and PE extracted paths (line)

The amount of residual noise in the PE extracted paths can be estimated by the difference in variance between the two distributions in Figure 7:

$$\sigma_r = \sqrt{\sigma_{PE}^2 - \sigma_{base}^2} \qquad (10)$$

where, σ_r is the residual noise in the PE extracted paths, σ_{base} is the noise relative to known true paths, and σ_{PE} is the noise measured relative to the PE extracted paths. The RMS noise values from the respective distributions are σ_{PE} = 0.425 nmi, σ_{base} = 0.424 nmi which implies a residual noise of σ_r = 0.03 nmi.

The close proximity in the shape of the noise distributions and the low estimated residual noise in the PE extracted paths indicate that the PE algorithm produced the desired outputs.

3. Conclusion

It has been shown that the PE algorithm reconstructs the actual aircraft paths from noisy target data to within a level of fidelity allowed by the effective target noise. The fact that the algorithm delivers segmented data (i.e. a non random component) in a geography-free coordinate system makes it suitable to define reference scenario data for testing and validation of ATM system components. Additional applications of the PE algorithm include computation of scenario metrics, and aircraft intent inference. By subtracting the wind velocity from the PE paths one should be able to determine those points were the true air speed changed (i.e. aircraft intent). The maneuvers and respective attributes provide useful scenario metrics to characterize patterns in the data.

References

[1] S.M. Green, S. Mondoloni, M. Paglione, S. Swierstra, R. Irvine, C. Garcia-Avello, Common Methodology and Resources for the Validation and Improvement of Trajectory Prediction Capabilities, *Eurocontrol Action Plan 16, White Paper*. (http://www.eurocontrol.int/care-tp/public/subsite_homepage/homepage.html)

[2] M. Basseville, I.V. Nikiforov, *Detection of Abrupt Changes - Theory and Application* (Englewood Cliffs, NJ: Prentice-Hall, 1993), http://www.irisa.fr/sisthem/kniga/

[3] W.S. Cleveland, Robust Locally Weighted Regression and Smoothing Scatterplots, *Journal of the American Statistical Association, 74*, 1979, 829-836.

[4] M. Paglione, R. Oaks, Determination of Horizontal and Vertical Phase of Flight in Recorded Air Traffic Data, *AIAA Guidance, Navigation, and Control*, Keystone, Colorado, 2006.

[5] R.J. Adler, *The Geometry of Random Fields* (New York: Wiley, 1981).

[6] H. Goldstain, *Classical mechanics* (Reading, MA: Addison-Wesley, 1980); and E.W. Weisstein, *Euler Angles*, from MathWorld (http://mathworld.wolfram.com/EulerAngles.html)

[7] N.J. Saleh, A.P. Smith, B.G. Sokkappa, The Stereographic Projection in the National Airspace System: Principles, Approximations and Errors, *MITRE preprint MTR-83W67,* May 1983.